How to cite: *Angew. Chem. Int. Ed.* **2024**, *63*, e202411753
doi.org/10.1002/anie.202411753

Hydrogen-Bonded Organic Frameworks | Hot Paper

Construction of Highly Porous and Robust Hydrogen-Bonded Organic Framework for High-Capacity Clean Energy Gas Storage

Jia-Xin Wang[+], Xu Zhang[+], Chenghao Jiang, Teng-Fei Zhang, Jiyan Pei, Wei Zhou, Taner Yildirim, Banglin Chen, Guodong Qian, and Bin Li**

Abstract: Development of highly porous and robust hydrogen-bonded organic frameworks (HOFs) for high-pressure methane and hydrogen storage remains a grand challenge due to the fragile nature of hydrogen bonds. Herein, we report a strategy of constructing the double-walled framework to target highly porous and robust HOF (ZJU-HOF-5a) for extraordinary CH_4 and H_2 storage. ZJU-HOF-5a features a minimized twofold interpenetration with double-walled structure, in which multiple supramolecular interactions are existed between the interpenetrated walls. This structural configuration can notably enhance the framework robustness while maintaining its high porosity, affording one of the highest gravimetric and volumetric surface areas of 3102 $m^2 g^{-1}$ and 1976 $m^2 cm^{-3}$ among the reported HOFs so far. ZJU-HOF-5a thus exhibits an extremely high volumetric H_2 uptake of 43.6 $g L^{-1}$ at 77 K/100 bar and working capacity of 41.3 $g L^{-1}$ under combined swing conditions (77 K/100 bar→160 K/5 bar), and also impressive methane storage performance with a 5–100 bar working capacity of 187 (or 159) cm^3 (STP) cm^{-3} at 270 K (or 296 K), outperforming most of the reported porous organic materials. Single-crystal X-ray diffraction studies on CH_4-loaded ZJU-HOF-5a reveal that abundant supramolecular binding sites combined with ultrahigh porosities account for its high CH_4 storage capacities. Combined with high stability, super-hydrophobicity, and easy recovery, ZJU-HOF-5a is placed among the most promising materials for H_2 and CH_4 storage applications.

Introduction

Carbon dioxide (CO_2) emissions are the primary driver of global climate change, which makes finding alternative sources of clean energy to replace conventional petroleum fuels to a level of utmost importance.[1] Methane (CH_4) and hydrogen (H_2) are both environmentally sustainable alternatives to gasoline for potential use as fuel for transportation sectors.[2] Methane represents a cleaner and cheaper fuel because of its abundant reserves, high research octane number (RON = 107), and less CO_2 emission than that of gasoline. Hydrogen is envisioned as an ideal green fuel because of its high energy density (33.3 kWh kg^{-1} vs 11.1 kWh kg^{-1} for gasoline) without CO_2 emission. However, the transportation and storage of hydrogen- and methane-powered vehicles currently require high-pressure compression (i.e., 700 bar for H_2 and 250 bar for CH_4).[3] The tank size, cost, and safety issues associated with high pressure restrict the usage of methane or hydrogen in light-duty vehicles with little space. In this context, the development of solid adsorbents for high densities of CH_4 or H_2 storage has received significant attention as an alternative to high-pressure compression.[4] To encourage research in this important field, the U.S. Department of Energy (DOE) launched a research program for the development of onboard storage and delivery systems for alternative fuels with ambitious goals for the transportation sectors.[5]

Realization of efficient adsorbents is of critical importance in targeting the safe and cost-effective storage of methane and hydrogen. During the last two decades, porous materials with high surface areas, such as metal–organic frameworks (MOFs),[6–9] activated carbons,[10] and covalent

[*] J.-X. Wang,[+] C. Jiang, T.-F. Zhang, J. Pei, Prof. G. Qian, Prof. B. Li
State Key Laboratory of Silicon and Advanced Semiconductor Materials
School of Materials Science and Engineering, Zhejiang University
Hangzhou 310027 (China)
E-mail: bin.li@zju.edu.cn

Prof. X. Zhang[+]
Jiangsu Engineering Laboratory for Environmental Functional Materials
School of Chemistry and Chemical Engineering, Huaiyin Normal University
Huaian 223300 (China)

Dr. W. Zhou, Dr. T. Yildirim
NIST Center for Neutron Research
National Institute of Standards and Technology
Gaithersburg, MD 20899–6102 (USA)

Prof. B. Chen
Fujian Provincial Key Laboratory of Polymer Materials
College of Chemistry & Materials Science, Fujian Normal University
Fuzhou 350007 (China)
E-mail: banglin.chen@fjnu.edu.cn

Prof. B. Chen
Key Laboratory of the Ministry of Education for Advanced Catalysis Materials
College of Chemistry and Materials Science, Zhejiang Normal University
Jinhua 321004 (China)

[+] These authors contributed equally to this work.

organic frameworks (COFs),[11,12] have been investigated intensively as promising adsorbents for the onboard storage of clean-energy gases, in which high surface area or pore volume plays an important role in their exceptional gas storage capacities. In this regard, the research on the emerging hydrogen-bonded organic frameworks (HOFs), assembled from organic molecules via intermolecular hydrogen bonds (H-bonds), has significantly lagged behind.[13–15] This is because the weak, flexible, and poorly directional nature of H-bonds makes HOF frameworks very difficult to stabilize and often collapse after the removal of solvent molecules. This drawback has made the construction of highly porous HOFs to be a long-standing challenge especially. Until now, there are only two reports of highly porous HOFs with Brunauer–Emmett–Teller surface areas (S_{BET}) larger than 3000 $m^2 g^{-1}$.[16] This challenge largely hampers the development of HOFs for CH_4 and H_2 storage under high pressure (e.g., 80 or 100 bar). By far, only two HOFs with moderate S_{BET} values (< 900 $m^2 g^{-1}$) have been developed to exhibit the relatively low CH_4 uptakes at 20 bar.[17] Even so, the intrinsic characteristics of H-bonds (weak, reversible, and flexible) enable porous HOFs to own some unique features that are different from MOFs, such as mild synthesis conditions, good solution processability, facile regeneration, and easy recovery by simple recrystallization.[18,19] Owing to the hydrophobic nature of organic moieties, HOFs generally exhibit better moisture insensitivity and repellency compared with that of MOFs.[20,21] These inherent merits make the development of highly porous HOFs be of particular interest for the storage of clean-energy gases.

For achieving high CH_4 and H_2 storage capacities of HOFs, it is very requisite to design highly porous HOF materials. The isoreticular linker expansion strategy has been well documented to be impactful for the construction of highly porous MOFs and COFs.[22,23] However, such direct linker extension to develop highly porous HOFs has often resulted in a high degree of framework interpenetration to stabilize the brittle porosity, which in turn reduces the open aperture sizes and surface areas.[24,25] Some progresses have been made to avoid framework interpenetration and thus create high porosities in HOFs.[16,26] For example, the energy–structure–function maps have been developed to guide the discovery of highly porous HOFs, leading to two non-interpenetrated HOFs that exhibit by far the record surface areas over 3400 $m^2 g^{-1}$.[16] However, their fragile H-bonded frameworks without interpenetration show low robustness and their ultrahigh porosities can only survive under harsh activation conditions, which largely hampers their practical applications. Evidently, high interpenetration in HOFs can improve the framework robustness, but would notably reduce the surface areas. Conversely, those large-pore HOFs without interpenetration often correlate to high porosity; however, their low structural robustness makes the establishment of ultrahigh surface area fail in most cases (Scheme 1). From the structural point of view, there commonly exists a mutual conflict between large surface area and high framework robustness in HOFs, making the development of ultraporous HOFs with high framework robustness remain a daunting challenge.

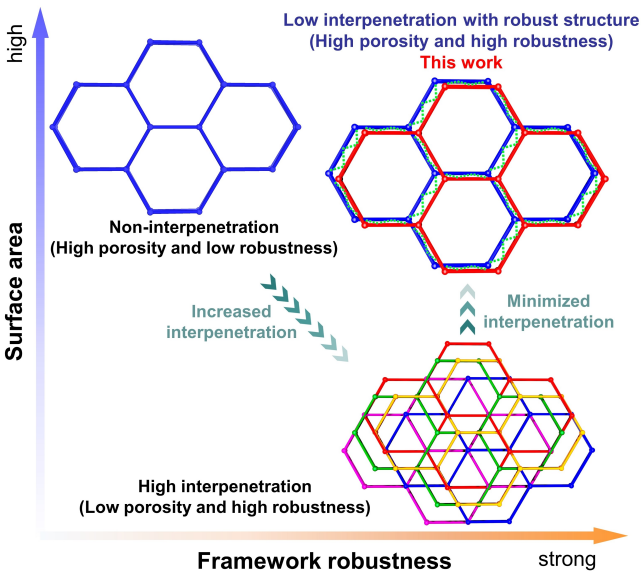

Scheme 1. The proposed strategy of constructing low interpenetration with robust structure (e.g., double-walled structure) in large-pore HOFs to target both large surface area and high framework robustness.

To overcome this challenge, it is highly important to minimize framework interpenetration while maintaining high pore robustness in large-pore HOFs. Recent studies have shown that the construction of double-walled framework in MOFs can notably improve framework robustness and stability,[27] since the short wall-to-wall distance enables the formation of some intermolecular interactions to strengthen the framework stability. Inspired by this finding, we reasoned that if we construct a large-pore HOF with twofold interpenetration to form a double-walled skeleton, it is highly potential to target both ultrahigh surface area and improved framework robustness because of its minimized interpenetration and robust double-walled structure (Scheme 1). With this in mind, we herein proposed and realized the construction of a double-walled HOF framework to achieve ultrahigh surface areas for high-capacity H_2 and CH_4 storage. By the self-assembly of a hexacarboxylate ligand of 2,4,6-triethylbenzene-1,3,5-isophthalic acid (H_6TEBIA), we developed a novel twofold interpenetrated HOF (termed as ZJU-HOF-5a), featuring the double-walled skeleton with large-pore channels. Single-crystal X-ray diffraction (SCXRD) studies revealed that multiple supramolecular interactions are formed between the interpenetrated walls, which can notably reinforce the large-pore and framework robustness. This led to the successful establishment of ultrahigh permanent porosities in ZJU-HOF-5a under the routine vacuum activation, resulting in one of the highest gravimetric and volumetric BET surface areas of 3102 $m^2 g^{-1}$ and 1976 $m^2 cm^{-3}$ by far. Such ultrahigh surface areas of ZJU-HOF-5a thus afford an extraordinary H_2 storage capacity of 43.6 $g L^{-1}$ at 77 K and 100 bar, with a high working capacity of 41.3 $g L^{-1}$ under combined temperature and pressure swing conditions (77 K/100 bar→160 K/

5 bar). This H_2 storage capacity is higher than most of the best-performing organic frameworks such as PAF-1 (38.3 $g L^{-1}$),[28] COF-1 (36.1 $g L^{-1}$),[11] and PPN-1 (5.7 $g L^{-1}$),[29] and even comparable to the promising MOFs including HKUST-1 (46 $g L^{-1}$) and NU-1500-Al (44.6 $g L^{-1}$).[4a,7a] Further, ZJU-HOF-5a also shows an impressive CH_4 storage performance with a total volumetric uptake of 232 (or 192) cm^3 (STP) cm^{-3} at 270 K (or 296 K) and 100 bar, and a 5–100 bar working capacity of 187 (or 159) cm^3 (STP) cm^{-3} at 270 K (or 296 K), which is also comparable to that of HKUST-1 (195 cm^3 (STP) cm^{-3}).[30] The primary CH_4 adsorption sites in ZJU-HOF-5a have been visually determined by the SCXRD experiments, revealing that abundant supramolecular binding sites and ultrahigh porosities synergistically contribute to its exceptional CH_4 storage capacities.

Results and Discussion

Previous literatures have clearly shown that self-assembly of the hexacarboxylate ligand of 2,4,6-trimethylbenzene-1,3,5-triylisophthalate (TMBTI) shows the potential to construct a three-dimensional (3D) rod-packing HOF framework with large pores.[31] However, the large-pore nature inevitably led to the formation of threefold and fourfold interpenetrated frameworks (Figure S1),[31] which can reinforce the framework robustness and thus establish the permanent porosities successfully. High interpenetration largely delimits their surface areas lower than 1500 $m^2 g^{-1}$. To improve the surface area, it is highly essential to reduce the number of framework interpenetration. For this purpose, we here designed and synthesized a novel hexacarboxylate ligand of H_6TEBIA by using more bulky ethyl groups to replace methyl groups, and utilized it to construct this kind of isomorphic rod-packing framework. It is speculated that the larger steric hindrance of ethyl groups may reduce the framework interpenetration for targeting higher surface area (Figure S1). The H_6TEBIA ligand was readily synthesized through a multistep reaction procedure (Scheme S1). Slow diffusion of n-hexane vapor into a THF solution of H_6TEBIA at room temperature for about one week afforded transparent HOF crystals (termed as ZJU-HOF-5) that are suitable for X-ray diffraction studies (Figure S5).

The SCXRD analysis revealed that ZJU-HOF-5 crystallizes in a hexagonal *P6/mcc* space group. As depicted in Figure 1a–1c, the steric hindrance of bulky ethyl groups indeed enables H_6TEBIA organic units to connect with each other through H-bonds to form the anticipative 3D rod-packing network. In a single network, the adjacent *meta*-benzenedicarboxylate motifs from different H_6TEBIA can form 1D infinite rod-shaped H-bonding chains along the *c* axis, which are further linked by the center phenyl ring to generate the 3D framework. As shown in Figure 1b, six discrete H_6TEBIA molecules form a six-membered ring with a large-pore channel of 18.6 Å. Such large-pore nature inevitably leads to interpenetration, while with a minimized twofold interpenetration in the resulting ZJU-HOF-5 due to the bulky ethyl groups (Figure 1c). Most importantly, this twofold interpenetration forms a unique double-walled skeleton in ZJU-HOF-5, affording large hexagonal pore channels with a size of 15.2 Å (Figure 1d), as further confirmed by the calculated geometric pore size distributions (PSD, Figure S7).[32] Unlike other interpenetrated frameworks that show obvious pore or aperture size reduction,[33] the twofold interpenetrated ZJU-HOF-5 exhibits a small decrease in the channel sizes due to its double-walled skeleton. Further, the two interpenetrated layers are in very close proximity to each other due to this double-walled structure, resulting in the formation of multiple supramolecular interactions between the two layers. As shown in Figure 1e, four O–H···O H-bonds are formed between two pairs of carboxylate acid, with the O–H···O distances of 3.303–3.319 Å. Moreover, multiple C–H···π van der Waals (vdW) interactions are also existed between the two layers (Figure 1e). These abundant supramolecular interactions can largely strengthen the robustness of the whole framework, so as to favor the establishment of ultrahigh porosity. Therefore, the unique double-walled structure of ZJU-HOF-5 can not only minimize the porosity or surface area reduction induced by the interpenetration, but also largely improve the framework robustness, enabling it to target simultaneously high surface area and framework robustness.

Before gas sorption analysis, the as-synthesized ZJU-HOF-5 was solvent-exchanged with dry n-hexane, and evacuated under the routine vacuum method to easily yield the fully activated ZJU-HOF-5a. PXRD patterns remain unchanged before and after the sample activation (Figure S8), confirming its high framework robustness. The ultrahigh permanent porosity of ZJU-HOF-5a was successfully established by nitrogen (N_2) gas sorption experiments at 77 K. As shown in Figure 1f, ZJU-HOF-5a adsorbs a large amount of N_2 (753 $cm^3 g^{-1}$) at 77 K and 1 bar, affording an exceptionally high gravimetric BET surface area of 3102 $m^2 g^{-1}$. This value is higher than all of the reported HOFs except T2-γ and TH5α (Table S1). Based on the determined crystallographic density of 0.637 $g cm^{-3}$, ZJU-HOF-5a also shows one of the highest volumetric surface areas with a value of 1976 $m^2 cm^{-3}$, notably larger than that of T2-γ (1411 $m^2 cm^{-3}$) and TH5α (1288 $m^2 cm^{-3}$).[16] Evidently, ZJU-HOF-5a represents the only HOF material with simultaneously high gravimetric and volumetric surface areas exceeding 3000 $m^2 g^{-1}$ and 1900 $m^2 cm^{-3}$ (Figure 1g), making it a very promising candidate for high-pressure hydrogen and methane storage.

The established ultrahigh surface areas in ZJU-HOF-5a encouraged us to examine its high-pressure methane and hydrogen sorption properties, measured at the National Institute for Standards and Technology (NIST). As shown in Figure 2a, ZJU-HOF-5a exhibits an excellent methane storage capacity with a total volumetric uptake of 232 and 192 cm^3 (STP) cm^{-3} at 270 K/100 bar and 296 K/100 bar, respectively, mainly attributed to its ultrahigh gravimetric and volumetric surface areas. The total CH_4 volumetric uptake of ZJU-HOF-5a at 296 K/100 bar surpasses that of most representative porous organic materials (Figure 2b and Table S2), such as PAF-1 (187 cm^3 (STP) cm^{-3} at 298 K/

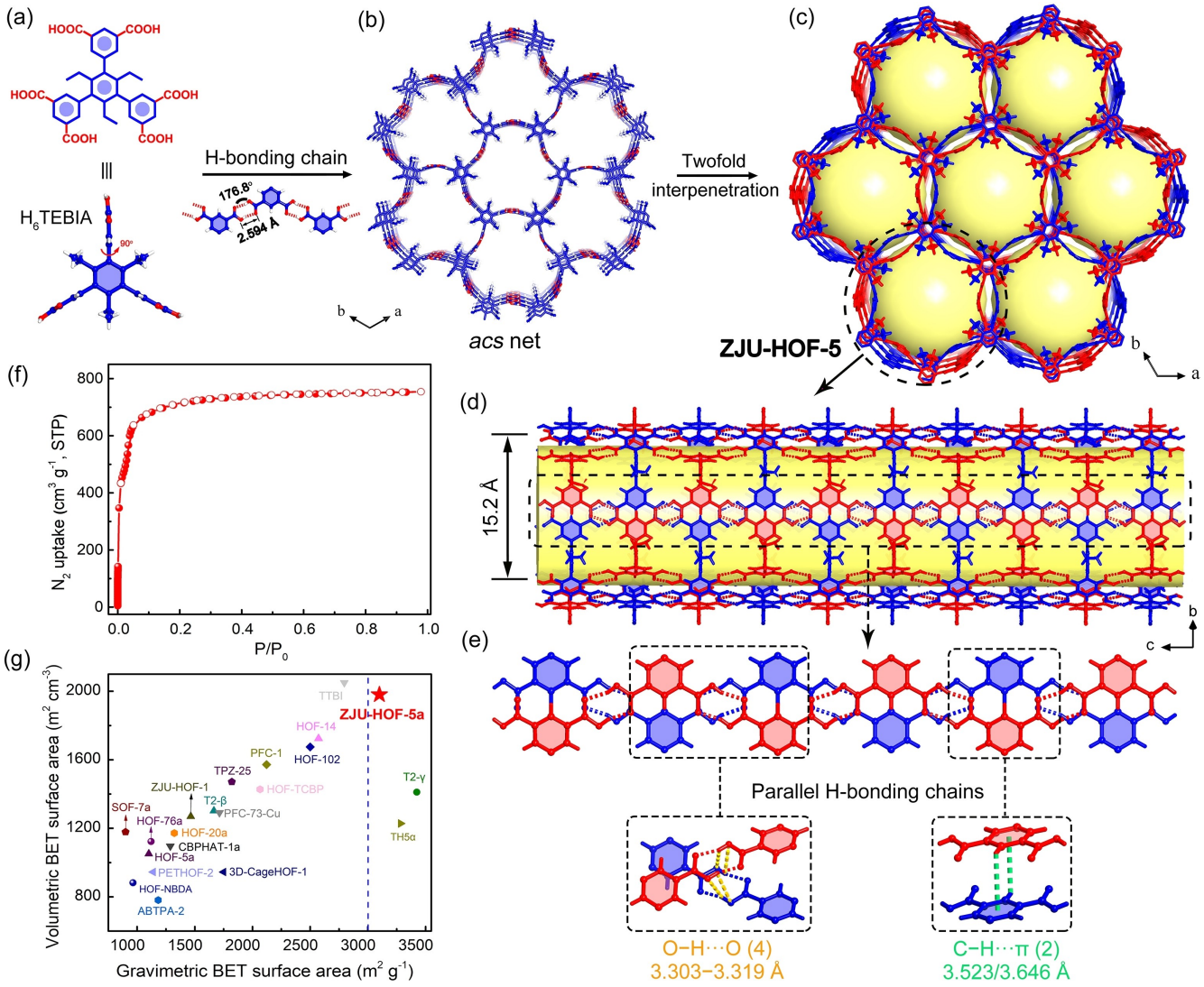

Figure 1. (a) The structure of the organic building unit. (b) The single network constructed by the organic units through O–H···O H-bonding chains. (c) The double-walled interpenetration in the single-crystal structure of ZJU-HOF-5. (d) The large 1D hexagonal pore channel of ZJU-HOF-5 with a diameter of 15.2 Å, viewed along the *a* axis. (e) Parallel H-bonding chains stabilized by multiple weak O–H···O H-bonds and C–H···π interactions. (f) N_2 sorption isotherms of ZJU-HOF-5a at 77 K. (g) Comparison of gravimetric and volumetric BET surface areas for the indicated porous HOFs. The crystal density of 0.637 g cm^{-3} was used to determine the volumetric values for ZJU-HOF-5a.

100 bar, based on simulated crystal density),[28a] COF-1 (89 cm^3 (STP) cm^{-3} at 298 K/80 bar),[11] KPOP-1 (128 cm^3 (STP) cm^{-3} at 298 K/80 bar),[34] and COP-150 (55 cm^3 (STP) cm^{-3} at 298 K/100 bar).[35] Such exceptional CH_4 storage capacity observed in ZJU-HOF-5a can also be explained by its high isosteric heats of adsorption (Q_{st}). As shown in Figure 2c, the experimental Q_{st} values for CH_4 adsorption are higher than most of the promising organic materials at the whole gas loadings. Its initial Q_{st} value is even comparable to those well-known MOFs with open metal sites (e.g., HKUST-1) (Figure S16 and Table S2), indicating the relatively strong interactions between the ZJU-HOF-5a framework and CH_4 molecule.

The methane storage working capacity (also called deliverable capacity), defined here as the difference in the amount of methane adsorbed between 100 and 5 bar, is more important than the total storage capacities, since it determines the driving range of vehicles powered by natural gas. We thus calculated the methane working capacity of ZJU-HOF-5a between 5 and 100 bar, affording a high value of 159 cm^3 (STP) cm^{-3} at 296 K. This capacity is higher than most of the representative organic frameworks like COF-1 (67 cm^3 (STP) cm^{-3}),[11] PAF-1 (156 cm^3 (STP) cm^{-3}),[28a] KPOP-1 (115 cm^3 (STP) cm^{-3}),[34] and COP-150 (48 cm^3 (STP) cm^{-3})[35] (Figure 2b and Table S2). Additionally, the working capacity of ZJU-HOF-5a can increase to 187 cm^3 (STP) cm^{-3} at 270 K, which is even comparable to the well-known HKUST-1 (195 cm^3 (STP) cm^{-3}) and Ni-MOF-74 (135 cm^3 (STP) cm^{-3}) under the same conditions.[30]

High-pressure hydrogen adsorption isotherms for ZJU-HOF-5a were further measured at 77, 160, and 296 K up to 100 bar, respectively. To our knowledge, this is the first

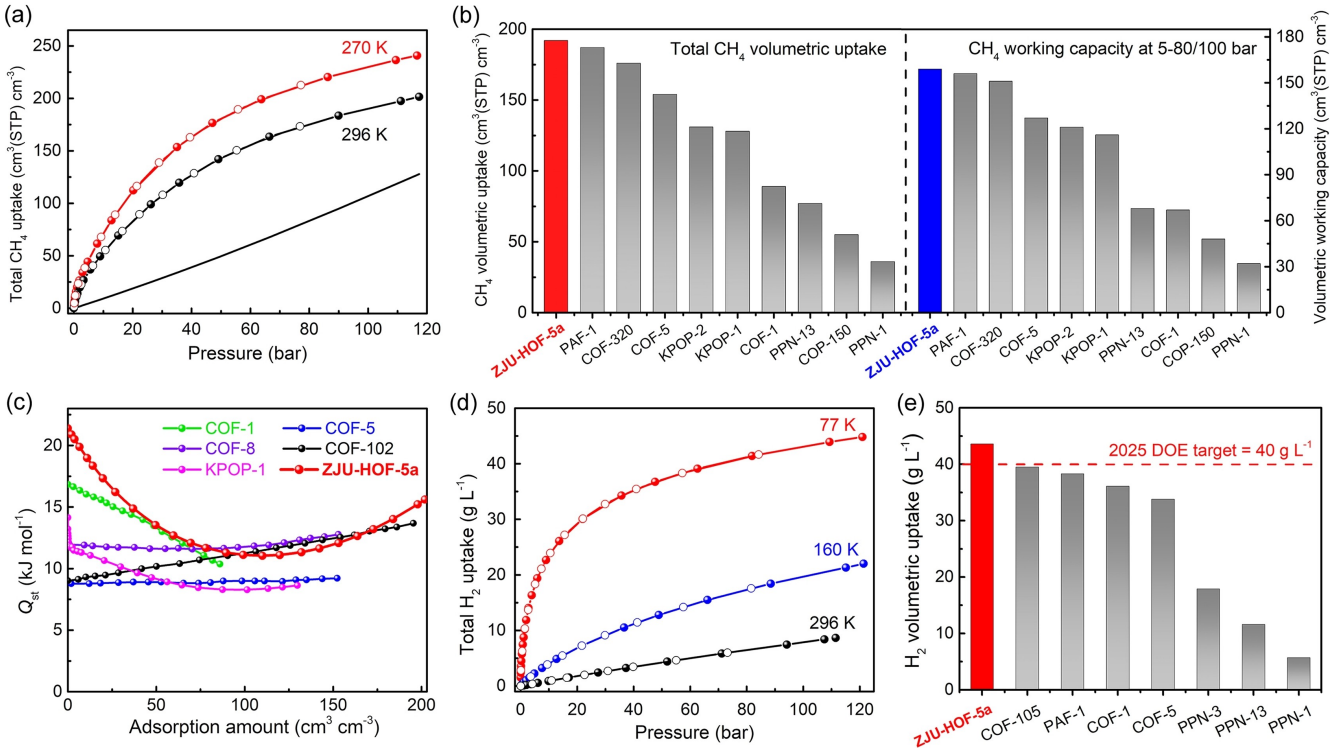

Figure 2. (a) Total volumetric CH_4 sorption isotherms of ZJU-HOF-5a at the indicated temperatures. Data of pure methane gas stored in a high-pressure gas tank is represented as a black solid curve. (b) Total methane volumetric uptakes (at room temperature and 80/100 bar, left) and working capacities (between 5 and 80/100 bar, right) for ZJU-HOF-5a and other representative porous organic materials. (c) The isosteric adsorption heat (Q_{st}) of CH_4 for ZJU-HOF-5a and other indicated porous materials. (d) Total volumetric hydrogen sorption isotherms for ZJU-HOF-5a at various temperatures. (e) Total volumetric hydrogen uptake of ZJU-HOF-5a at 77 K compared with some top-performing porous organic materials.

example of HOFs that was systematically evaluated for hydrogen storage at different temperatures. As presented in Figure 2d, ZJU-HOF-5a shows a very high total hydrogen volumetric uptake of 43.6 $g\,L^{-1}$ at 77 K/100 bar. This total volumetric uptake is notably higher than most of the benchmark organic materials (Figure 2e and Table S3), including PAF-1 (38.3 $g\,L^{-1}$),[28b] COF-1 (36.1 $g\,L^{-1}$),[11] and PPN-1 (5.7 $g\,L^{-1}$),[29] and even comparable to that of some benchmark MOFs such as NU-1500-Al (46.8 $g\,L^{-1}$) and HKUST-1 (49 $g\,L^{-1}$).[4a,7a] The H_2 storage working capacity was calculated by taking the difference between the total amount of H_2 uptake at 77 K/100 bar and 160 K/5 bar, subscribing to the tank design criteria studied by the HSECoE.[36] ZJU-HOF-5a displays an extraordinary H_2 working capacity of 41.3 $g\,L^{-1}$ under the combined swing conditions of 77 K/100 bar→160 K/5 bar, satisfying the 2025 tank design target proposed by DOE.[5b] This working capacity is even comparable to the well-known HKUST-1 (46.0 $g\,L^{-1}$) and NU-1500-Al (44.6 $g\,L^{-1}$).[4a,7a] All these results suggest that ZJU-HOF-5a can be placed among the most promising materials for high-capacity methane and hydrogen storage.

To better understand the origin of the high storage capacities observed in ZJU-HOF-5a, we performed the SCXRD experiments on gas-loaded ZJU-HOF-5a to determine the gas binding sites. Despite extensive attempts, we were not able to determine the hydrogen adsorption sites in the H_2-loaded structure because of the small X-ray cross-section of hydrogen atoms. Fortunately, the SCXRD data of CH_4-loaded ZJU-HOF-5a (CH_4@ZJU-HOF-5a) were successfully collected and determined at 120 K (Table S4).[37] As shown in Figure 3a, ZJU-HOF-5a was found to exhibit three primary binding sites (site-I, site-II, and site-III) for the adsorbed CH_4 molecules, all of which are located around the organic building units. The site-I binding site is located at the pore pockets formed between the interpenetrated layers (Figure 3b and 3c), in which each CH_4 molecule interacts with the two stacked phenyl rings and four carboxylic oxygen atoms through four C–H···π (H···π, 2.834(2)–3.999(3) Å) and four O–H···O (H···O, 3.279(3)–4.218(2) Å) interactions. There also exist multiple C–H···C (H···C, 3.341(3)–3.897(2) Å) supramolecular interactions between CH_4 and four surrounding ethyl groups (Table S5), indicating that the incorporated ethyl groups also contribute to improving the CH_4 binding affinity. Both site-II and site-III binding sites are located at the large pore channels (Figure 3b), all of which are in close proximity to the surrounding organic linkers. Each CH_4 molecule adsorbed at site-II or site-III forms multiple C–H···π, O–H···O, and C–H···C interactions with the adjacent phenyl rings, carboxylic oxygen atoms, and ethyl groups, respectively (Figure 3d and Table S5). We note that a full occupancy of these

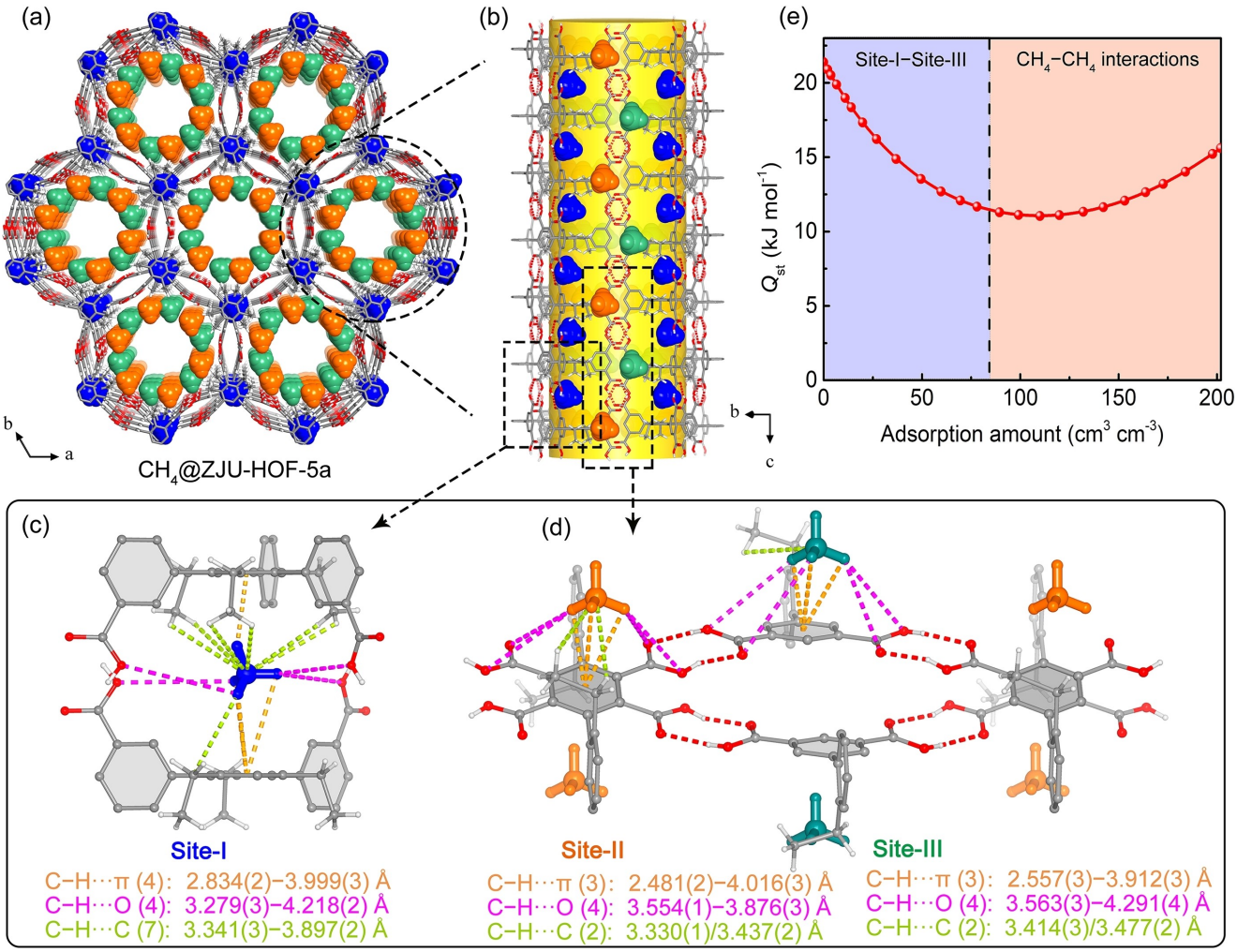

Figure 3. Single-crystal structure of CH_4-loaded ZJU-HOF-5a (a) viewed along *c* axis and (b) viewed along *a* axis, revealing three types of binding sites for CH_4 molecules. (c) and (d) Illustration of multiple supramolecular interactions between the framework and CH_4 molecules in ZJU-HOF-5a at (c) Site-I, (d) Site-II and Site-III. The hydrogen atoms of methane were generated geometrically. (e) The CH_4 adsorption heat (Q_{st}) for ZJU-HOF-5a along with the CH_4 adsorption amount.

adsorption sites corresponds to a gas adsorption capacity of about 80 $cm^3 cm^{-3}$, which is equivalent to the experimental CH_4 uptake amount (83.5 $cm^3 cm^{-3}$) at 296 K and 20 bar. Therefore, during the low-pressure CH_4 adsorption below 20 bar, multiple supramolecular interactions between CH_4 molecules and the host framework dominate the CH_4 adsorption amount. With the pressure increased, the CH_4–CH_4 interaction might start to kick in to dominate the uptake of methane at high pressures. This can be well supported by the calculated Q_{st} curve at the whole pressure range (Figure 3e), in which the Q_{st} value for CH_4 adsorption gradually decreases with gas loading to 100 $cm^3 cm^{-3}$ due to the occupancy of these binding sites. Whereafter, a gradual increase occurs at high loadings after 100 $cm^3 cm^{-3}$, which can be probably attributed to the attractive CH_4–CH_4 interactions, as well confirmed by previous studies on some large-pore MOFs.[6a,7b,c] Taken together, the abundant supramolecular binding sites combined with ultrahigh surface areas mainly account for its extraordinary methane storage capacities.

In practical applications, commercial gases commonly contain trace amounts of water vapor,[4,38] which may slowly poison adsorption sites or degrade the framework over a long period. This phenomenon was often encountered in many MOFs. For example, some high-performing MOFs (e.g., MOF-74, UTSA-76, and HKUST-1) are commonly sensitive to humidity or show high water uptake to result in competitive adsorption, thus suffering from gas storage capacity reduction or structure decomposition.[6d,30,38] Thus, the practical conditions require adsorbents with extremely high framework robustness and low water competitive adsorption. We first examine the chemical stability of ZJU-HOF-5 by exposing the samples to different chemical environments for two days, including water, aqueous solutions of pH 1 and 10, and 12 M HCl. The framework of ZJU-HOF-5 can retain its structural integrity without any phase change and loss of crystallinity, as revealed by the

PXRD patterns and SEM images (Figure 4a, S20 and S21). N_2 adsorption isotherms after the above treatments are very close to that of the pristine sample (Figure 4b), further confirming its ultrahigh stability. In addition, ZJU-HOF-5 also exhibits good thermal stability up to 200 °C, as indicated by the almost unchanged variable-temperature PXRD patterns (Figure S22). To effectively avoid the negative effect of water vapor, ideal materials should have not only high water stability but also low water uptake to minimize the competitive adsorption of water. Due to the hydrophobic nature of HOFs, ZJU-HOF-5a exhibits a negligible adsorption of water (0.059 $g\,g^{-1}$) at 298 K even under 95 % RH (Figure 4c), which is much lower than that of HKUST-1 (0.63 $g\,g^{-1}$) and Ni-MOF-74 (0.48 $g\,g^{-1}$). This negligible water uptake can mostly avoid the negative effect of moisture, making this HOF material more practical than many MOFs for clean energy gas storage in realistic applications. Moreover, the ZJU-HOF-5 sample also exhibits excellent recovery ability due to the reversible nature of H-bonds. As shown in Figure 4d and S27, the damaged framework by mechanical grinding can be easily recovered by immersing into the growth solution or completely regenerated by recrystallization, with N_2 uptakes comparable to that of the pristine sample. Overall, the excellent storage capacities, high stability, negligible water uptake, and easy recovery make this HOF material as one of the most promising materials for methane and hydrogen storage applications.

Conclusion

To summarize, we have successfully proposed and demonstrated a strategy of designing double-walled framework in large-pore HOFs to achieve ultrahigh surface areas for the effective storage of methane and hydrogen gases. A highly porous and robust HOF material with twofold interpenetration (ZJU-HOF-5a) was reported, wherein the twofold interpenetration led to the desired double-walled structure. This unique architecture can not only minimize the degree of interpenetration to maintain high surface areas, but also improve the framework robustness by forming multiple supramolecular interactions between the interpenetrated layers. The ultrahigh porosities were thereby established in ZJU-HOF-5a, affording one of the highest gravimetric and volumetric BET surface areas (3102 $m^2\,g^{-1}$ and 1976 $m^2\,cm^{-3}$) among the reported HOFs by far. ZJU-HOF-5a achieves the best CH_4 and H_2 volumetric total uptakes and working capacities among all the reported HOFs, which are higher than most of the benchmark PAFs and COFs, and even comparable to that of the well-known MOFs (e.g., HKUST-1). The primary CH_4 adsorption sites have been visualized within ZJU-HOF-5a by gas-loaded SCXRD studies, revealing that its excellent CH_4 storage capacities are mainly attributed to the synergistic effect of abundant supramolecular binding sites and ultrahigh surface areas. The combined advantages of the exceptional storage capacities, notably stability, high hydrophobicity, and easy repairability, make this material as a very promising material for clean energy gas storage applications. This work not only provides an effective strategy to design highly porous and robust HOFs for ultrahigh surface areas, but also highlights the bright potential of developing HOFs for clean energy gas storage in the future.

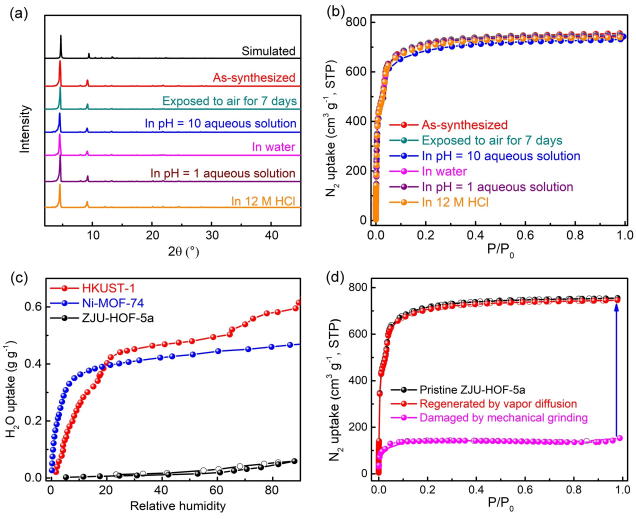

Figure 4. (a) PXRD patterns and (b) N_2 adsorption isotherms of ZJU-HOF-5a sample after the treatment with different conditions. (c) Water vapor adsorption isotherms of HKUST-1, Ni-MOF-74, and ZJU-HOF-5a at 298 K. (d) 77 K N_2 adsorption isotherms of pristine ZJU-HOF-5a and the samples after being damaged by mechanical grinding and regenerated by vapor diffusion.

Acknowledgements

This research was partially supported by the Zhejiang Provincial Natural Science Foundation of China (No. LR22E030003), the National Natural Science Foundation of China (52073251 and 22275064), Natural Science Foundation for Colleges and Universities in Jiangsu Province (21KJA530003), and the Science and Technology Department of Zhejiang Province (2022C01225). We also acknowledge the Shanghai Synchrotron Radiation Facility (SSRF) for single-crystal X-ray diffraction data collection.

Conflict of Interest

The authors declare no conflict of interest.

Data Availability Statement

The data that support the findings of this study are available in the supplementary material of this article.

Keywords: porous materials · supramolecular binding · methane · hydrogen storage · clean energy

[1] S. Chu, Y. Cui, N. Liu, *Nat. Mater.* **2017**, *16*, 16–22.

[2] T. He, P. Pachfule, H. Wu, Q. Xu, P. Chen, *Nat. Rev. Mater.* **2016**, *1*, 16059.

[3] K. V. Kumar, K. Preuss, M.-M. Titirici, F. Rodríguez-Reinoso, *Chem. Rev.* **2017**, *117*, 1796–1825.

[4] a) P. García-Holley, B. Schweitzer, T. Islamoglu, Y. Liu, L. Lin, S. Rodriguez, M. H. Weston, J. T. Hupp, D. A. Gómez-Gualdrón, T. Yildirim, O. K. Farha, *ACS Energy Lett.* **2018**, *3*, 748–754; b) B. Li, H.-M. Wen, W. Zhou, J. Q. Xu, B. Chen, *Chem* **2016**, *1*, 557–580; c) D. Yuan, W. Lu, D. Zhao, H.-C. Zhou, *Adv. Mater.* **2011**, *23*, 3723–3725.

[5] a) Methane opportunities for vehicular energy (MOVE), advanced research project agency-energy, U. S. Department of Energy, Funding Opportunity No. DE-FOA-0000672, https://arpa-e-foa.energy.gov/Default.aspx?Search=DE-FOA-0000672; b) Target explanation document: onboard hydrogen storage for light-duty fuel cell vehicles, U. S. Department of Energy, https://www.energy.gov/sites/default/files/2017/05/f34/fcto_targets_onboard_hydro_storage_explanation.pdf.

[6] a) S. Ma, D. Sun, J. M. Simmons, C. D. Collier, D. Yuan, H.-C. Zhou, *J. Am. Chem. Soc.* **2008**, *130*, 1012–1016; b) H. Furukawa, N. Ko, Y. B. Go, N. Aratani, S. B. Choi, E. Choi, A. Ö. Yazaydin, R. Q. Snurr, M. O'Keeffe, J. Kim, O. M. Yaghi, *Science* **2010**, *329*, 424–428; c) C. E. Wilmer, O. K. Farha, T. Yildirim, I. Eryazici, V. Krungleviciute, A. A. Sarjeant, R. Q. Snurr, J. T. Hupp, *Energy Environ. Sci.* **2013**, *6*, 1158–1163; d) B. Li, H.-M. Wen, H. Wang, H. Wu, M. Tyagi, T. Yildirim, W. Zhou, B. Chen, *J. Am. Chem. Soc.* **2014**, *136*, 6207–6210.

[7] a) Z. Chen, P. Li, R. Anderson, X. Wang, X. Zhang, L. Robison, L. R. Redfern, S. Moribe, T. Islamoglu, D. A. Gómez-Gualdrón, T. Yildirim, J. F. Stoddart, O. K. Farha, *Science* **2020**, *368*, 297–303; b) Y. Yan, D. I. Kolokolov, I. da Silva, A. G. Stepanov, A. J. Blake, A. Dailly, P. Manuel, C. C. Tang, S. Yang, M. Schröder, *J. Am. Chem. Soc.* **2017**, *139*, 13349–13360; c) D. Alezi, Y. Belmabkhout, M. Suyetin, P. M. Bhatt, Ł. J. Weseliński, V. Solovyeva, K. Adil, I. Spanopoulos, P. N. Trikalitis, A.-H. Emwas, M. Eddaoudi, *J. Am. Chem. Soc.* **2015**, *137*, 13308–13318; d) H.-M. Wen, B. Li, L. Li, R.-B. Lin, W. Zhou, G. Qian, B. Chen, *Adv. Mater.* **2018**, *30*, 1704792.

[8] a) Y. He, W. Zhou, G. Qian, B. Chen, *Chem. Soc. Rev.* **2014**, *43*, 5657–5678; b) Y. Bai, Y. Dou, L.-H. Xie, W. Rutledge, J.-R. Li, H.-C. Zhou, *Chem. Soc. Rev.* **2016**, *45*, 2327–2367; c) J. J. Perry IV, J. A. Permana, M. J. Zaworotko, *Chem. Soc. Rev.* **2009**, *38*, 1400–1417; d) K. Suresh, D. Aulakh, J. Purewal, D. J. Siegel, M. Veenstra, A. J. Matzger, *J. Am. Chem. Soc.* **2021**, *143*, 10727–10734.

[9] a) J. A. Mason, J. Oktawiec, M. K. Taylor, M. R. Hudson, J. Rodriguez, J. E. Bachman, M. I. Gonzalez, A. Cervellino, A. Guagliardi, C. M. Brown, P. L. Llewellyn, N. Masciocchi, J. R. Long, *Nature* **2015**, *527*, 357–361; b) Z. Chen, K. O. Kirlikovali, K. B. Idrees, M. C. Wasson, O. K. Farha, *Chem* **2022**, *8*, 693–716; c) K. Koupepidou, V. I. Nikolayenko, D. Sensharma, A. A. Bezrukov, M. Vandichel, S. J. Nikkhah, D. C. Castell, K. A. Oyekan, N. Kumar, A. Subanbekova, W. G. Vandenberghe, K. Tan, L. J. Barbour, M. J. Zaworotko, *J. Am. Chem. Soc.* **2023**, *145*, 10197–10207; d) K. Nath, K. R. Wright, A. Ahmed, D. J. Siegel, A. J. Matzger, *J. Am. Chem. Soc.* **2024**, *146*, 10517–10523.

[10] a) M. E. Casco, M. Martínez-Escandell, E. Gadea-Ramos, K. Kaneko, J. Silvestre-Albero, F. Rodríguez-Reinoso, *Chem. Mater.* **2015**, *27*, 959–964; b) N. Albeladi, L. S. Blankenship, R. Mokaya, *Energy Environ. Sci.* **2024**, *17*, 3060–3076.

[11] a) S. S. Han, H. Furukawa, O. M. Yaghi, W. A. Goddard, *J. Am. Chem. Soc.* **2008**, *130*, 11580–11581; b) H. Furukawa, O. M. Yaghi, *J. Am. Chem. Soc.* **2009**, *131*, 8875–8883.

[12] Y.-B. Zhang, J. Su, H. Furukawa, Y. Yun, F. Gándara, A. Duong, X. Zou, O. M. Yaghi, *J. Am. Chem. Soc.* **2013**, *135*, 16336–16339.

[13] a) D. Venkataraman, S. Lee, J. Zhang, J. S. Moore, *Nature* **1994**, *371*, 591–593; b) M. Simard, D. Su, J. D. Wuest, *J. Am. Chem. Soc.* **1991**, *113*, 4696–4698; c) R.-B. Lin, Y. He, P. Li, H. Wang, W. Zhou, B. Chen, *Chem. Soc. Rev.* **2019**, *48*, 1362–1389; d) I. Hisaki, C. Xin, K. Takahashi, T. Nakamura, *Angew. Chem. Int. Ed.* **2019**, *58*, 11160–11170.

[14] a) Y. He, S. Xiang, B. Chen, *J. Am. Chem. Soc.* **2011**, *133*, 14570–14573; b) A. Karmakar, R. Illathvalappil, B. Anothumakkool, A. Sen, P. Samanta, A. V. Desai, S. Kurungot, S. K. Ghosh, *Angew. Chem. Int. Ed.* **2016**, *55*, 10667–10671.

[15] a) H. Yamagishi, H. Sato, A. Hori, Y. Sato, R. Matsuda, K. Kato, T. Aida, *Science* **2018**, *361*, 1242–1246; b) T. Takeda, M. Ozawa, T. Akutagawa, *Angew. Chem. Int. Ed.* **2019**, *58*, 10345–10352; c) F. Hu, C. Liu, M. Wu, J. Pang, F. Jiang, D. Yuan, M. Hong, *Angew. Chem. Int. Ed.* **2017**, *56*, 2101–2104.

[16] a) A. Pulido, L. Chen, T. Kaczorowski, D. Holden, M. A. Little, S. Y. Chong, B. J. Slater, D. P. McMahon, B. Bonillo, C. J. Stackhouse, A. Stephenson, C. M. Kane, R. Clowes, T. Hasell, A. I. Cooper, G. M. Day, *Nature* **2017**, *543*, 657–664; b) C. E. Shields, X. Wang, T. Fellowes, R. Clowes, L. Chen, G. M. Day, A. G. Slater, J. W. Ward, M. A. Little, A. I. Cooper, *Angew. Chem. Int. Ed.* **2023**, e202303167.

[17] a) W. Yang, A. Greenaway, X. Lin, R. Matsuda, A. J. Blake, C. Wilson, W. Lewis, P. Hubberstey, S. Kitagawa, N. R. Champness, M. Schröder, *J. Am. Chem. Soc.* **2010**, *132*, 14457–14469; b) J. Lü, C. Perez-Krap, M. Suyetin, N. H. Alsmail, Y. Yan, S. Yang, W. Lewis, E. Bichoutskaia, C. C. Tang, A. J. Blake, R. Cao, M. Schröder, *J. Am. Chem. Soc.* **2014**, *136*, 12828–12831.

[18] a) B. Wang, R.-B. Lin, Z. Zhang, S. Xiang, B. Chen, *J. Am. Chem. Soc.* **2020**, *142*, 14399–14416; b) W. Liang, F. Carraro, M. B. Solomon, S. G. Bell, H. Amenitsch, C. J. Sumby, N. G. White, P. Falcaro, C. J. Doonan, *J. Am. Chem. Soc.* **2019**, *141*, 14298–14305; c) J. Gao, Y. Cai, X. Qian, P. Liu, H. Wu, W. Zhou, D.-X. Liu, L. Li, R.-B. Lin, B. Chen, *Angew. Chem. Int. Ed.* **2021**, *60*, 20400–20406; d) Y. Chen, Y. Yang, Y. Wang, Q. Xiong, J. Yang, S. Xiang, L. Li, J. Li, Z. Zhang, B. Chen, *J. Am. Chem. Soc.* **2022**, *144*, 17033–17040.

[19] a) P. Li, M. R. Ryder, J. F. Stoddart, *Acc. Mater. Res.* **2020**, *1*, 77–87; b) Z.-J. Lin, S. A. R. Mahammed, T.-F. Liu, R. Cao, *ACS Cent. Sci.* **2022**, *8*, 1589–1608; c) Y. Zhou, C. Chen, R. Krishna, Z. Ji, D. Yuan, M. Wu, *Angew. Chem. Int. Ed.* **2023**, *62*, e202305041; d) C. Jiang, J.-X. Wang, D. Liu, E. Wu, X.-W. Gu, X. Zhang, B. Li, B. Chen, G. Qian, *Angew. Chem. Int. Ed.* **2024**, *63*, e202404734.

[20] a) I. Hisaki, Y. Suzuki, E. Gomez, B. Cohen, N. Tohnai, A. Douhal, *Angew. Chem. Int. Ed.* **2018**, *57*, 12650–12655; b) B. Han, H. Wang, C. Wang, H. Wu, W. Zhou, B. Chen, J. Jiang, *J. Am. Chem. Soc.* **2019**, *141*, 8737–8740; c) X. Song, Y. Wang, C. Wang, D. Wang, G. Zhuang, K. O. Kirlikovali, P. Li, O. K. Farha, *J. Am. Chem. Soc.* **2022**, *144*, 10663–10687; d) X. Zhang, L. Li, J.-X. Wang, H.-M. Wen, R. Krishna, H. Wu, W. Zhou, Z.-N. Chen, B. Li, G. Qian, B. Chen, *J. Am. Chem. Soc.* **2020**, *142*, 633–640; e) H. Li, C. Chen, Q. Li, X. J. Kong, Y. Liu, Z. Ji, S. Zou, M. Hong, M. Wu, *Angew. Chem. Int. Ed.* **2024**, *63*, e202401754.

[21] a) X.-Z. Luo, X.-J. Jia, J.-H. Deng, J.-L. Zhong, H.-J. Liu, K.-J. Wang, D.-C. Zhong, *J. Am. Chem. Soc.* **2013**, *135*, 11684–11687; b) T.-H. Chen, I. Popov, W. Kaveevivitchai, Y.-C. Chuang, Y.-S. Chen, O. Daugulis, A. J. Jacobson, O. Š Miljanić, *Nat. Commun.* **2014**, *5*, 5131; c) X.-L. Lv, S. Yuan, L.-H. Xie, H. F. Darke, Y. Chen, T. He, C. Dong, B. Wang, Y.-Z. Zhang, J.-R. Li, H.-C. Zhou, *J. Am. Chem. Soc.* **2019**, *141*, 10283–10293; d) J. Li, P. Liu, Y. Chen, J. Zhou, J. Li, J. Yang,

D. Zhang, J. Li, L. Li, *J. Am. Chem. Soc.* **2023**, *145*, 19707–19714.
[22] a) H. Deng, S. Grunder, K. E. Cordova, C. Valente, H. Furukawa, M. Hmadeh, F. Gándara, A. C. Whalley, Z. Liu, S. Asahina, H. Kazumori, M. O'Keeffe, O. Terasaki, J. F. Stoddart, O. M. Yaghi, *Science* **2012**, *336*, 1018–1023; b) B. Li, H.-M. Wen, Y. Cui, W. Zhou, G. Qian, B. Chen, *Adv. Mater.* **2016**, *28*, 8819–8860; c) H. Wang, Y. Liu, J. Li, *Adv. Mater.* **2020**, *32*, 2002603; d) W. Fan, X. Zhang, Z. Kang, X. Liu, D. Sun, *Coord. Chem. Rev.* **2021**, *443*, 213968.
[23] a) S.-Y. Ding, W. Wang, *Chem. Soc. Rev.* **2013**, *42*, 548–568; b) X. Feng, X. Ding, D. Jiang, *Chem. Soc. Rev.* **2012**, *41*, 6010–6022; c) S. Tao, H. Xu, Q. Xu, Y. Hijikata, Q. Jiang, S. Irle, D. Jiang, *J. Am. Chem. Soc.* **2021**, *143*, 8970–8975; d) C. He, S. Tao, R. Liu, Y. Zhi, D. Jiang, *Angew. Chem. Int. Ed.* **2024**, *63*, e202403472.
[24] a) C. A. Zentner, H. W. H. Lai, J. T. Greenfield, R. A. Wiscons, M. Zeller, C. F. Campana, O. Talu, S A FitzGerald, J. L. C. Rowsell, *Chem. Commun.* **2015**, *51*, 11642–11645; b) I. Bassanetti, S. Bracco, A. Comotti, M. Negroni, C. Bezuidenhout, S. Canossa, P. P. Mazzeo, L. Marchió, P. Sozzani, *J. Mater. Chem. A* **2018**, *6*, 14231–14239; c) Y. Yang, L. Li, R.-B. Lin, Y. Ye, Z. Yao, L. Yang, F. Xiang, S. Chen, Z. Zhang, S. Xiang, B. Chen, *Nat. Chem.* **2021**, *13*, 933–939.
[25] a) Y.-L. Li, E. V. Alexandrov, Q. Yin, L. Li, Z.-B. Fang, W. Yuan, D. M. Proserpio, T.-F. Liu, *J. Am. Chem. Soc.* **2020**, *142*, 7218–7224; b) Q. Zhu, J. Johal, D. E. Widdowson, Z. Pang, B. Li, C. M. Kane, V. Kurlin, G. M. Day, M. A. Little, A. I. Cooper, *J. Am. Chem. Soc.* **2022**, *144*, 9893–9901; c) P. Li, Z. Chen, M. R. Ryder, C. L. Stern, Q.-H. Guo, X. Wang, O. K. Farha, J. F. Stoddart, *J. Am. Chem. Soc.* **2019**, *141*, 12998–13002; d) P. Li, P. Li, M. R. Ryder, Z. Liu, C. L. Stern, O. K. Farha, J. F. Stoddart, *Angew. Chem. Int. Ed.* **2019**, *58*, 1664–1669.
[26] a) M. Mastalerz, I. M. Oppel, *Angew. Chem. Int. Ed.* **2012**, *51*, 5252–5255; b) M. I. Hashim, H. T. M. Le, T.-H. Chen, Y.-S. Chen, O. Daugulis, C.-W. Hsu, A. J. Jacobson, W. Kaveevivitchai, X. Liang, T. Makarenko, O. Š Miljanić, I. Popovs, H. V. Tran, X. Wang, C.-H. Wu, J. I. Wu, *J. Am. Chem. Soc.* **2018**, *140*, 6014–6026; Miljanić, I. Popovs, H. V. Tran, X. Wang, C.-H. Wu, J. I. Wu, *J. Am. Chem. Soc.* **2018**, *140*, 6014–6026; c) Q. Yin, P. Zhao, R.-J. Sa, G.-C. Chen, J. Lü, T.-F. Liu, R. Cao, *Angew. Chem. Int. Ed.* **2018**, *57*, 7691–7696; d) I. Hisaki, Y. Suzuki, E. Gomez, Q. Ji, N. Tohnai, T. Nakamura, A. Douhal, *J. Am. Chem. Soc.* **2019**, *141*, 2111–2121; e) K. Ma, P. Li, J. H. Xin, Y. Chen, Z. Chen, S. Goswami, X. Liu, S. Kato, H. Chen, X. Zhang, J. Bai, M. C. Wasson, R. R. Maldonado, R. Q. Snurr, O. K. Farha, *Cell Rep. Phys. Sci.* **2020**, *1*, 100024.
[27] a) T. He, X.-J. Kong, Z.-X. Bian, Y.-Z. Zhang, G.-R. Si, L.-H. Xie, X.-Q. Wu, H. Huang, Z. Chang, X.-H. Bu, M. J. Zaworotko, Z.-R. Nie, J.-R. Li, *Nat. Mater.* **2022**, *21*, 689–695; b) L. Hu, W. Wu, M. Hu, L. Jiang, D. Lin, J. Wu, K. Yang, *Nat. Commun.* **2024**, *15*, 3204.
[28] a) S. Bracco, D. Piga, I. Bassanetti, J. Perego, A. Comotti, P. Sozzani, *J. Mater. Chem. A* **2017**, *5*, 10328–10337; b) T. Ben, H. Ren, S. Ma, D. Cao, J. Lan, X. Jing, W. Wang, J. Xu, F. Deng, J. M. Simmons, S. Qiu, G. Zhu, *Angew. Chem. Int. Ed.* **2009**, *48*, 9457–9460.
[29] W. Lu, D. Yuan, D. Zhao, C. I. Schilling, O. Plietzsch, T. Muller, S. Bräse, J. Guenther, J. Blümel, R. Krishna, Z. Li, H.-C. Zhou, *Chem. Mater.* **2010**, *22*, 5964–5972.
[30] Y. Peng, V. Krungleviciute, I. Eryazici, J. T. Hupp, O. K. Farha, T. Yildirim, *J. Am. Chem. Soc.* **2013**, *135*, 11887–11894.
[31] a) X. Zhang, J.-X. Wang, L. Li, J. Pei, R. Krishna, H. Wu, W. Zhou, G. Qian, B. Chen, B. Li, *Angew. Chem. Int. Ed.* **2021**, *60*, 10304–10310; b) F.-A. Guo, K. Zhou, J. Liu, H. Wang, J. Li, *Precis. Chem.* **2023**, *1*, 524–529.
[32] S. Bhattacharya, K. E. Gubbins, *Langmuir* **2006**, *22*, 7726–7731.
[33] a) R. Zhu, J. Ding, L. Jin, H. Pang, *Coord. Chem. Rev.* **2019**, *389*, 119–140; b) X. Guan, Q. Fang, Y. Yan, S. Qiu, *Acc. Chem. Res.* **2022**, *55*, 1912–1927.
[34] J. Jia, Z. Chen, H. Jiang, Y. Belmabkhout, G. Mouchaham, H. Aggarwal, K. Adil, E. Abou-Hamad, J. Czaban-Jóźwiak, M. R. Tchalala, M. Eddaoudi, *Chem* **2019**, *5*, 180–191.
[35] V. Rozyyev, D. Thirion, R. Ullah, J. Lee, M. Jung, H. Oh, M. Atilhan, C. T. Yavuz, *Nat. Energy* **2019**, *4*, 604–611.
[36] D. J. Siegel, B. Hardy, HSECoE Team. Engineering an adsorbent-based hydrogen storage system: What have we learned? https://energy.gov/sites/prod/files/2015/02/f19/fcto_h2_storage_summit_siegel.pdf.
[37] Deposition numbers 2363470 (for ZJU-HOF-5) and 2133280 (for CH_4@ZJU-HOF-5a) contain the supplementary crystallographic data for this paper. These data are provided free of charge by the joint Cambridge Crystallographic Data Centre and Fachinformationszentrum Karlsruhe Access Structures service.
[38] a) V. Rozyyev, C. T. Yavuzl, *Chem* **2017**, *3*, 719–721; b) T. A. Makal, J.-R. Li, W. Lu, H.-C. Zhou, *Chem. Soc. Rev.* **2012**, *41*, 7761–7779; c) J. A. Mason, M. Veenstra, J. R. Long, *Chem. Sci.* **2014**, *5*, 32–51.

Manuscript received: June 22, 2024
Accepted manuscript online: August 13, 2024
Version of record online: October 29, 2024